Journal of Applied Sciences

ISSN 1812-5654

science alert

ANSInet
an open access publisher
http://ansinet.com

Journal of Applied Sciences 11 (12): 2214-2219, 2011
ISSN 1812-5654 / DOI: 10.3923/jas.2011.2214.2219

Mixed-Mode Fracture Analysis of Aluminum Alloy 5083 Subjected to Four Point Bending

[1]R. Ravichandaran and [2]G. Thanigaiyarasu
[1]Department of Mechanical Engineering, Arunai Engineering College,
Tiruvannamalai, Tamil Nadu, 606603, India
[2]Engineering Design Division, College of Engineering Guindy Campus,
Anna University Chennai, Chennai, 600025, India

Abstract: The aim of this research study is to evaluate the stress intensity factors of aluminum 5083 of different thickness subjected to mixed-mode loading. Asymmetric four point bend specimen is a convenient test configuration for estimating mixed-mode fracture properties of engineering materials. In this study, experimental and numerical studies of mixed-mode I/II fracture behavior are presented. The mixed-mode stress intensity factors of the material are evaluated for different location of crack from the middle of the span. Influence of the location of crack from the mean position on the fracture toughness is studied for different specimen thickness. The results obtained are compared with that of the finite element analysis. It is shown that the experimentally determined Stress Intensity Factors goes well with the numerical results.

Key words: Four point bend specimen, mixed-mode, stress intensity factor, strain energy release rate, aluminum alloy

INTRODUCTION

In recent years, mixed-mode crack growth and investigation of fracture have gained a lot of insight. There was much research work for the fracture under mixed-mode loading conditions. Khan and Khraisheh (2000) have proposed failure criteria, which govern mixed-mode fracture.

There were many works concerning the brittle fracture in mixed-mode in the literature (Ayatollahi and Torabi, 2010; Jun *et al*., 2006; Saghafi *et al*., 2010; Ayatollahi and Torabi, 2009). However, there is no much research work concerning mixed-mode fracture of ductile materials.

There are some theoretical methods (Shahani and Tabatabaei, 2008; Decreuse *et al*., 2009) for evaluating the fracture behavior under mixed-mode I/II loading conditions in four point bend specimen. However, there is a lack of potential method to calculate mode I and mode II SIF values for specimens with different thickness. Furthermore, there is only few works (Zimmermann *et al*., 2009) to calculate strain energy release rate in a specimen subjected to asymmetric four point bending.

According to Zimmermann *et al*. (2009), when a specimen with crack is loaded with mixed-mode configuration the crack driving force can be described in terms of critical strain energy release rate G which can be defined in terms of applied SIF values, K_I, K_{II} and K_{III} by the following expression:

$$G = \frac{K_I^2}{E'} + \frac{K_{II}^2}{E'} + \frac{K_{III}^2}{E'} \quad (1)$$

Where,

$$E' = \frac{E}{(1-\nu^2)} \quad (2)$$

Where:
E = Modulus of elasticity (Pa)
v = Poisson's ratio

For mixed-mode loading, the mode-mixity of the applied force-specimen configuration can be described by a parameter called phase angle, β:

$$\beta = \tan^{-1}\left[\frac{K_{II}}{K_I}\right] \quad (3)$$

The objective of this research work is to determine the stress intensity factors of aluminum 5083 of different thickness subjected to mixed-mode loading and compare the values with failure criterion like Maximum Hoop Stress(MHS) Criterion. Four point bend specimen has been used for this work.

MATERIALS AND METHODS

This work was carried out during June to December 2010 at Department of Mechanical Engineering, Arunai

Corresponding Author: R. Ravichandaran, Arunai Engineering College, Tiruvannamalai, Tamil Nadu-606603, India
Tel: 00919442367155

Engineering College, Tiruvannamalai, Tamil Nadu, India. Aluminum 5083 is the material used for our analysis. The composition of aluminum 5083 grade is given in Table 1. Four Point Bend (FPB) specimen was used to evaluate mode I and mode II SIFs. The simple geometry and loading set up, the convenient precracking of a specimen and the ability of introducing mode mixities (from pure mode I to pure mode II) are among the advantages of FPB specimen. For studying mixed-mode fracture in each test specimen, the more I and mode II SIFs (K_I and K_{II}) should be known. In the forthcoming sections, the SIF values of the four-point-bend specimen are determined by the finite element analysis. Then mixed-mode fracture is investigated experimentally for an aluminum alloy specimen using the FPB specimen.

Figure 1 shows a schematic drawing of an asymmetric Four Point Bend (FPB) specimen. The support is divided into two roller supports at the bottom and at the top. When the crack is perfectly at the mid-span of the specimen, the problem is a pure mode II problem. A little consideration will show that the bending moment in the middle of the specimen is zero and so mode II is the only induced mode in the specimen. By moving the crack away from the middle of the specimen, the bending moment can be increased and mode I can be created. The shear force will create mode II so that the combination of the two modes (mode I and mode II), mode mixity will be created:

$$Q = \frac{F(L-d)}{L} \quad (4)$$

$$M = S.Q. \quad (5)$$

Where:
Q = Shear force
M = Bending moment
F = Applied force
S = Crack distance from mid-span

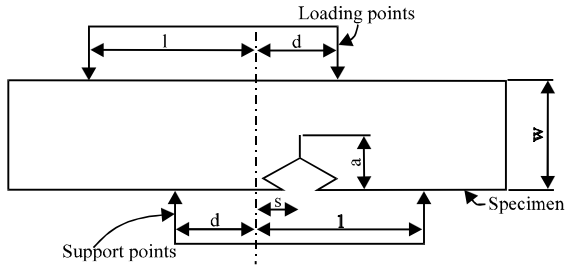

Fig. 1: Four point bend specimen with asymmetric loading

Table 1: Composition of Aluminum 5083

Si	Cu	Fe	Mn	Mg	Zn	Cr	Ti	Al
0.35	0.10	0.25	0.4	4.2	0.25	0.05	0.15	Balance

L and d- are the distances from loading points to mid-span as shown in Fig. 1.

Shahani and Tabatabaei (2008) have calculated the SIFs of modes I and II for a four-point bend specimen in terms of geometric functions.

MATERIALS AND METHODS

All the specimens were tested on a standard servo hydraulic universal testing machine of 100 kN (kilo Newton) capacity. A calibrated load cell and a crack opening displacement gauge were used.

The specimens were divided into three groups based on their thickness (6.35, 9.6 and 12.7 mm). They are called 1T, 1.5T and 2T, respectively. In each group, five specimens were taken and the notches were fabricated in such a way that the crack distance from the mid-span varies to be 0.0, 2.5, 5.0, 7.5 and 10.0 mm). Then, all the specimens were loaded in a four point bend set up to find the pop in load. The pop-in loads which were experimentally observed, were used to calculate the SIFs as given by He and Hutchinson (2000) and Shahani and Tabatabaei (2008).

Using the shear force and bending moment calculated from the Eq. 4 and 5, the SIFs in mode I and II can be obtained from Eq. 6 and 7, respectively:

$$K_I = \frac{6SQ}{W^2}\sqrt{\pi a}F_I(a/W) \quad (6)$$

$$K_{II} = \frac{Q}{W^{1/2}}\frac{(a/W)^{3/2}}{(1-a/W)^{1/2}}F_{II}(a/W) \quad (7)$$

where, functions F_I and F_{II} were used by Shahani and Tabatabaei (2008) as polynomial functions:

$$F_I = 1.121(a/W) + 3.74(a/W)^2 + 3.873(a/W)^3 - 19.05(a/W)^4 + 22.55(a/W)^5, 0 < a/W < 0.7 \quad (8)$$

$$F_{II} = 7.264 - 9.37(a/W) + 2.74(a/W)^2 + 1.87(a/W)^3 - 1.04(a/W)^4, 0 < a/W < 1 \quad (9)$$

Where:
a = Crack length
W = Specimen width

The formulae for K_I and K_{II} given by Ming and Sakai (1996), Shahani and Tabatabaei (2008) and Zimmermann *et al.* (2009) differ by some factors as follows:

$$(K_I)_{MingLi} = 4.49\,(K_I)_{Zimmermann} = 3.12\,(K_I)_{Shahani} \quad (10)$$

$$(K_{11})_{MingLi} = 3.029\,(K_{II})_{Zimmermann} = 1.01\,(K_{II})_{Shahani} \quad (11)$$

RESULTS

The maximum tangential stress criteria (Ayatollahi and Aliha, 2007) otherwise called Maximum Hoop Stress (MHS) criteria is well known theory for mixed-mode fracture. Based on this criteria, fracture in a cracked body under mixed-mode I/II loading will occur in a specific direction when the tangential quantities in this direction reaches its critical value. For example, the onset of fracture for a cracked body subjected to mixed-mode loading takes place according to the maximum tangential criterion when:

$$K_{Ic} \le \cos\left(\frac{\theta_c}{2}\right)\left[K_I \cos^2\left(\frac{\theta_c}{2}\right) - \frac{3}{2}\sin(\theta_c)\right] \quad (12)$$

All specimens of all three groups were fatigue precracked to a/W = 0.5 in a three point bend setup. The pop in loads were noted for each experiment and listed in Table 2. The experimental SIF values of mode I, II and combined mode I/II fractures are calculated from these pop in loads.

From the observation of experimental results, Stress Intensity Factor (SIF) values were affected by two factors, one, the crack distance from the middle of the specimen and the other, the thickness of the specimen. The experimental K_I/K_{Ic} vs K_{II}/K_{Ic} of combined mode I/II fracture experiments are shown in Fig. 2-4.

The values of strain energy release rates are calculated from Eq. 2. Results showing the variation of strain energy release rate (G) per unit thickness is plotted against mode-mixity, β and shown in Fig. 5. The G values are drastically reduced in 2T thick plates compared to the cases of 1.5T and 1T plates.

The SIF values for diverse mode-mixities and for different thickness are compared in Fig. 6 and 7. The mode I SIF values show a downward trend and in mode II, they show an upward trend against the mode-mixity β.

Finite Element Method (FEM): In order to validate the experimental results, the model is analysed using finite element method. The specimen was discretized using ANSYS commercial code with 8-node isoparametric elements. The analysis was performed in the elastic state and a plane stress condition was assumed to be imposed on the problem. In all analyses, a total of 10500 to 11500 elements and 32000 to 33500 nodes were used.

A plane stress condition was set with thickness option. A modulus of elasticity was set 70000 MPa. Singular quarter point elements were used around the crack tip to model the crack tip singularity. The finite element mesh is shown in Fig. 8.

The specimen was analyzed for 15 different configurations and load conditions. These 15 geometries correspond to the 15 cases of the experiments, five states of crack distances from the middle of the specimen and three thicknesses.

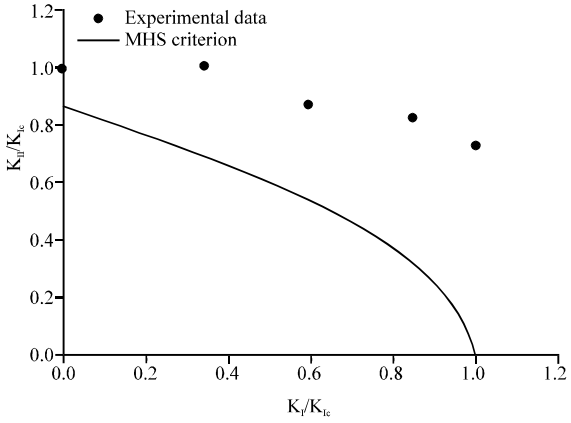

Fig. 2: K_{II}/K_{Ic} vs K_I/K_{Ic} envelopes of 2T specimens

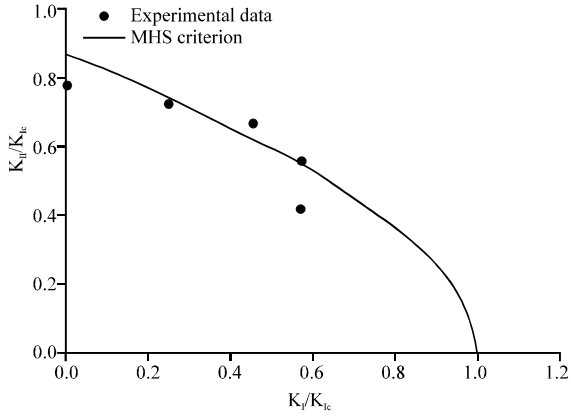

Fig. 3: K_{II}/K_{Ic} vs K_I/K_{Ic} fracture envelopes of 1.5T specimens

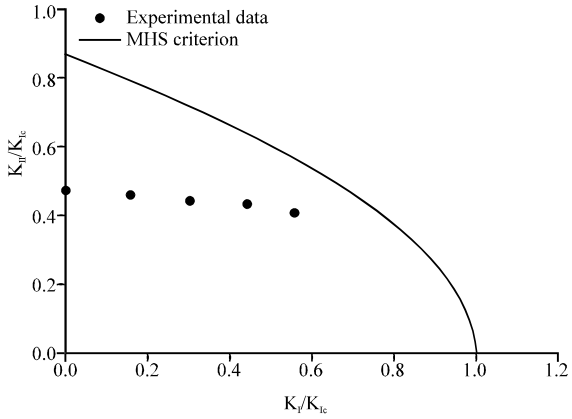

Fig. 4: K_{II}/K_{Ic} vs K_I/K_{Ic} fracture envelopes of 1T specimens

The SIF values were calculated using the ANSYS program. A sample set of results obtained from FEM is compared with that of experimental results in Fig. 9 and 10.

Figure 1 illustrates the specimen used for this research work. In Fig. 2, the stress intensity factor/fracture values in mode I and mode II are drawn as an envelope and compared with Maximum Hoop Stress (MHS) criteria for 2T thickness(12.7 mm). In Fig. 3, the stress intensity factor / fracture toughness values in mode I and mode II are compared with Maximum Hoop Stress (MHS) criteria for 1.5T thickness (9.6 mm). In Fig. 4, the stress intensity factor/fracture toughness values in I and mode II are compared with Maximum Hoop Stress (MHS) criteria for 1T thickness (6.35 mm).

Figure 5 details the variation of critical Strain Energy Release Rate (SERR) with respect to different mode-mixity (β) values for various thickness. Figure 6 explains the variation of stress intensity factor in mode I with the change in mode-mixity (β) for three different

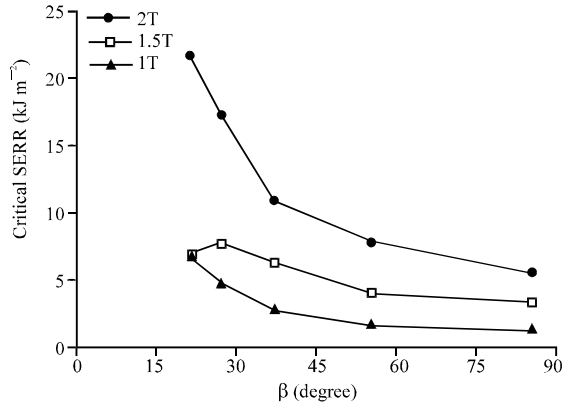

Fig. 5: Critical strain energy release rate (G) vs mode-mixity (β)

Table 2: Specimen geometry and loading details

Specimen No.	Thickness (mm)	Max load (N)	Crack distance (mm)	*SIF in mode 1 ---- (Mpa sqrt m) ---	*SIF in mode 2
	B	P	S	K_I	K_{II}
4	12.70	74331	0.0	0.00	68.23
3	12.70	75031	2.5	43.40	65.30
5	12.70	65184	5.0	79.50	57.80
6	12.70	61751	7.5	108.60	51.20
7	12.70	54614	10.0	139.20	44.76
11	9.60	43625	0.0	0.00	48.23
12	9.60	40789	2.5	32.30	45.32
13	9.60	37407	5.0	57.30	44.10
14	9.60	31294	7.5	70.80	37.40
15	9.60	23432	10.0	79.80	24.30
21	6.35	17568	0.0	0.00	43.90
22	6.35	17104	2.5	19.30	36.50
23	6.35	16498	5.0	38.90	27.98
24	6.35	16093	7.5	54.30	28.30
25	6.35	15191	10.0	73.40	31.20

*SIF: Stress intensity factor

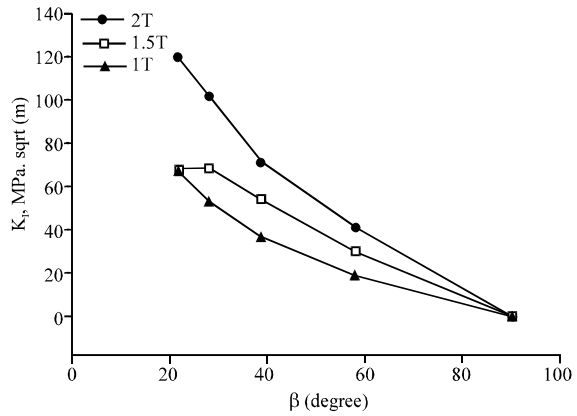

Fig. 6: The variation of K_I vs mode-mixity, β

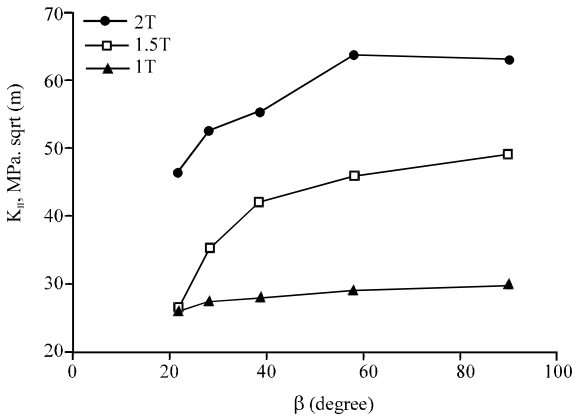

Fig. 7: The variation of K_{II} vs mode-mixity, β

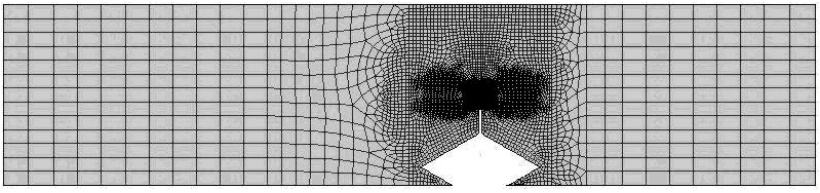

Fig. 8: Finite element mesh of the test specimen

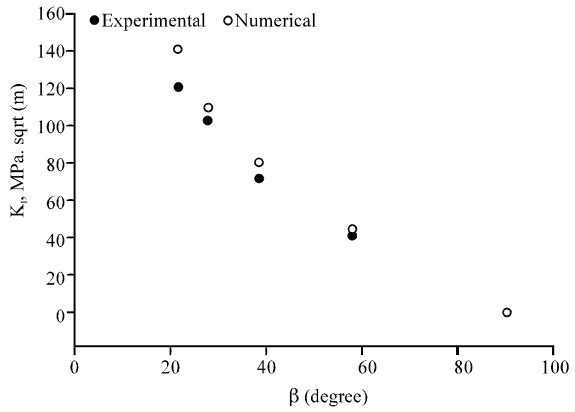

Fig. 9: Comparison of mode I SIF, K_I (Numerical) and K_I (experimental) corresponds to 2T thickness

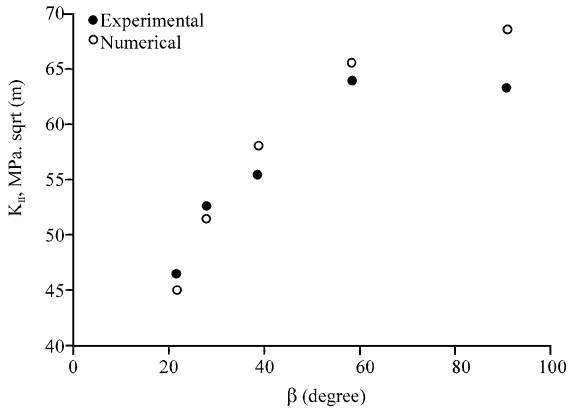

Fig. 10: Comparison of mode II SIF values, K_{II} (Numerical) and K_{II} (experimental) corresponds to 2T specimens

thickness of the specimens. Figure 7 sketches the variation of stress intensity factor in mode II with the change in mode-mixity (β) for three different thicknesses of the specimens. Figure 8 depicts the finite element model and mesh generated based on the specimen sketch. Figure 9 compares the stress intensity factor K_I of numerical (ANSYS software) and experimental values for different mode mixity. Figure 10 shows the comparison of the stress intensity factor K_{II} of numerical (ANSYS software) and experimental values for different mode mixity.

DISCUSSION

Some of the outcomes of this report are the mixed-mode stress intensity factor, energy release rate and crack propagation length of aluminum alloy grade 5083. The fracture envelopes Fig. 2 and 3 for 2 and 1.5T specimens are comparable to that of the literature available (Chao and Shu, 1997). But, in the case of 1T specimens, all the failure points are within the fracture envelope.

The fracture envelopes of 1.5T specimens are in agreement with Saghafi *et al.* (2010), Maccagno and Knott (1989) and Ming and Sakai (1996). However, the fracture envelopes of 2T specimens go out of the MHC criterion envelope which is in contradiction with Ming and Sakai (1996). At the same time, 1T specimens are well within the MHC criterion.

The mode I stress intensity factors decrease with the increase in crack distance from the mid-span (mode-mixity). But, the variation of mode II stress intensity factors with the increase in crack distance from the mid-span is increasing to an upper value and stabilizes. This is also supported by He and Hutchinson (2000) and Shahani and Tabatabaei (2008, 2009). The growing rend of mode II stress intensity factors with the increase in mode-mixity (β), is supported also by Mendelsohn *et al.* (2001). As well, he decreasing bbehavior of mode I stress intensity factor with mode-mixity is observed by Carmona *et al.* (2007) on reinforced concrete specimens and Ayatollahi and Aliha (2007) on brittle rock specimens.

Critical SERR obtained experimentally go well with the results of transverse orientation of Zimmermann *et al.* (2009, 2010) but it contracts with longitudinal directional results of Zimmermann *et al.* (2009) . The G values in near the mode I is the highest and near mode II, the lowest.

These results may be considered to have significant consequences as to how the relevance and applicability of fracture mechanics are viewed and as applied to aluminum alloys.

CONCLUSION

The mixed-mode properties stress intensity factors and critical strain energy release rate of the aluminum alloy 5083 were calculated and plotted against the crack distance from the mid-span of the speciemen.

The failure of the material (Al 5083 alloy) was compared with maximum hoop stress theory. It has been found that the upper bound value of SIF in mode I (K_I) is always greater than SIF in mode II (K_{II}) by 20-45%. Hence, in FPB test, aluminum alloy 5083 is weaker in mode I than in mode II.

The experimental results are compared to that of numerical results found from ANSYS program and found to be close when the crack is nearer to the mid-span.

ACKNOWLEDGMENT

The authors wish to acknowledge the help and support provided by BiSS Research, Bangalore, India.

REFERENCES

Ayatollahi, M.R. and A.R. Torabi, 2009. A criterion for brittle fracture in U-notched components under mixed-mode loading. Eng. Fract. Mech., 76: 1883-1896.

Ayatollahi, M.R. and A.R. Torabi, 2010. Investigation of mixed-mode brittle fracture in rounded-tip V-notched components. Eng. Fract. Mech., 77: 3087-3104.

Ayatollahi, M.R. and M.R.M. Aliha, 2007. Fracture toughness study for a brittle rock subjected to mixed mode I/II loading. Int. J. Rock Mech. Min. Sci., 44: 617-624.

Carmona, J.R., G. Ruiz and J.R. del Viso, 2007. Mixed-mode crack propagation through reinforced concrete. Eng. Fract. Mech., 74: 2788-2809.

Chao, Y.J. and L. Shu, 1997. On the failure of cracks under mixed-mode loads. Int. J. Fract., 87: 201-223.

Decreuse, P.Y., S. Pommier, L. Gentot and S. Pattofatto, 2009. History effect in fatigue crack growth under mixed-mode loading conditions. Int. J. Fatigue, 31: 1733-1741.

He, M.Y. and J.W. Hutchinson, 2000. Asymmetric four-point crack specimen. J. Applied Mech., 67: 207-209.

Jun, C., J. Xu and Y. Mutoh, 2006. A general mixed-mode brittle fracture criterion for cracked materials. Eng. Fract. Mech., 73: 1249-1263.

Khan, S.M.A. and M.K. Khraisheh, 2000. Analysis of mixed mode crack initiation angles under various loading conditions. Eng. Fract. Mech., 67: 397-419.

Maccagno, T.M. and J.F. Knott, 1989. The fracture behaviour of PMMA in mixed modes I and II. Eng. Fract. Mech., 34: 65-86.

Mendelsohn, D.A., T.S. Gross, L.J. Young, F. Chen and R.U. Goulet, 2001. Geometry and load fixture effects in the four-point-bend mixed mode fracture specimen. Eng. Fract. Mech., 68: 587-604.

Ming, L. and M. Sakai, 1996. Mixed-mode fracture of ceramics in asymmetric four-point bending: Effect of crack face grain interlocking- bridging. J. Am. Ceram. Soc., 79: 2718-2726.

Saghafi, H., M.R. Ayatollahi and M. Sistaninia, 2010. A modified MTS criterion (MMTS) for mixed-mode fracture toughness assessment of brittle materials. Mater. Sci. Eng. A, 527: 5624-5630.

Shahani, A.R. and S.A. Tabatabaei, 2008. Computation of mixed-mode stress intensity factors in a four point bend specimen. Applied Math. Modell., 32: 1281-1288.

Shahani, A.R. and S.A. Tabatabaei, 2009. Effect of T-stress on the fracture of a four point bend specimen. Mater. Design, 30: 2630-2635.

Zimmermann, E.A., M.E. Launey, H.D. Barth and R.O. Ritchie, 2009. Mixed-mode fracture of human cortical bone. Biomaterials, 30: 5877-5884.

Zimmermann, E.A., M.E. Launey and R.O. Ritchie, 2010. The significance of crack-resistance curves to the mixed-mode fracture toughness of human cortical bone. Biomaterials, 31: 5297-5308.